A LETTERS JOURNAL EXPLORING
THE FRONTIERS OF PHYSICS

LETTER

Anomalous Fano resonance of massive Dirac particle through a time-dependent barrier

To cite this article: Cunxi Zhang *et al* 2015 *EPL* **110** 61001

A LETTERS JOURNAL EXPLORING THE FRONTIERS OF PHYSICS

June 2015

EPL, **110** (2015) 61001
doi: 10.1209/0295-5075/110/61001

www.epljournal.org

Anomalous Fano resonance of massive Dirac particle through a time-dependent barrier

CUNXI ZHANG[1,2,3], JIE LIU[1,4] and LIBIN FU[1,4(a)]

[1] *Institute of Applied Physics and Computational Mathematics - Beijing 100088, China*
[2] *School of Naval Architecture and Ocean Engineering, Zhejiang Ocean University - Zhoushan 316022, China*
[3] *Key Laboratory of Oceanographic Big Data Mining Application of Zhejiang Province, Zhejiang Ocean University Zhoushan, Zhejiang 316022, China*
[4] *HEDPS, Center for Applied Physics and Technology, Peking University - 100084 Beijing, China*

received 27 March 2015; accepted in final form 12 June 2015
published online 1 July 2015

PACS 11.80.-m – Relativistic scattering theory
PACS 03.65.Pm – Relativistic wave equations
PACS 03.65.Xp – Tunneling, traversal time, quantum Zeno dynamics

Abstract – As is well known Fano resonance arises from the interference between a localized state and a continuum state. Using the standard Floquet theory and the scattering matrix method, we study theoretically the massive Dirac particle transmission over a quantum barrier with an oscillating field. It is found that the massive relativistic particles can generate not only normal Fano resonance in the transmission due to the interference between a localized state (bound state) and the continuum state, but also anomalous Fano resonance due to the interference between a delocalized state (extended state) and the continuum state. The dependence of line shapes on driving parameters for these two kinds of Fano resonances is quite different. For normal Fano resonance the asymmetry parameter is approximately proportional to a power law of the amplitude of the oscillating field, while for the anomalous Fano resonance the asymmetry parameters change slightly with different oscillation amplitudes. In practice, the anomalous Fano resonance can be identified by observing asymmetry parameters in experiment.

Introduction. – Fano resonance [1], an intriguing quantum phenomenon originating from the interference between a continuum energy band and an embedded discrete energy level, has been extensively studied in different systems [2]. The striking signature of Fano resonance is its unique asymmetric lineshape which is distinctively different from the conventional symmetric resonance. As a fundamental phenomenon, Fano resonance finds a broad range of applications, such as sensing and switching [3].

The interest in the investigation of Fano resonance in a relativistic environment is greatly motivated by the exotic properties and easy experimental implementations of Dirac quasiparticles in graphene and/or artificial graphene [4]. These systems provide promising platforms to test the fundamental relativistic physics, such as Zitterbewegung [5,6] and Klein tunnelling [7]. The experimental [8,9] and theoretical [10,11] studies on few-layer graphene demonstrate that Fano resonance is an important probe to reveal the properties of graphene.

In this paper, we theoretically study the transportation of a massive Dirac particle in an oscillating potential barrier. Due to the oscillating barrier, the Fano resonance of the massless [12,13] and massive [14] Dirac particle develops to a set of photon-assisted sidebands. The Klein tunneling is shown to be suppressed by the irradiation of a strong laser field, and the bound states may offer discrete energy levels to confine the Dirac particle in the barrier [13,14]. Here we adopt the interferometer geometry which is realized by a time-periodic barrier and study the Fano resonance with the Floquet theory. We find that, when the energy of the incident particle matches the resonance condition, the interferences between the continuum and bound state will lead to the appearance of the asymmetric normal Fano resonance. However, when the frequency of the oscillating barrier is higher than the mass of the particle (frequency and mass in energy unit), one will find new Fano resonances in the transmission coefficient. They belong to supercritical resonances because positive-energy states connect to a negative-energy state, and the incident particle's energy matches a negative-energy

(a)E-mail: lbfu@iapcm.ac.cn

state's frequency. The new resonances correspond to the interference of the continuum and extended state, the latter one is the negative-energy solution of the Dirac equation. The new kind of resonances is quite different from the normal Fano resonance. For normal Fano resonances, the asymmetry parameter decreases as the power of the oscillation amplitude, however for the anomalous Fano resonance the asymmetry parameters remain approximately constants with the increase of the oscillation amplitude.

Model. – We consider a Dirac particle transmitting through a one-dimensional time-periodic potential barrier which extends from $-a/2$ to $a/2$ (see fig. 1(a)), that is

$$V(x,t) = \begin{cases} V_0 + V\cos(\omega t), & -a/2 \le x \le a/2, \\ 0, & \text{otherwise.} \end{cases} \quad (1)$$

Here V_0 is the static barrier height, V and ω denote the amplitude and the frequency of the applied oscillating field, respectively. A relativistic particle motion with mass m may be described by the time-dependent Dirac equation

$$i\hbar\frac{\partial}{\partial t}\Phi(x,t) = \hat{H}\Phi(x,t) \quad (2)$$

with the Hamiltonian

$$\hat{H} = -i\hbar c\sigma_x\frac{\mathrm{d}}{\mathrm{d}x} + V(x,t) + \sigma_z mc^2, \quad (3)$$

where c denotes the (effective) velocity of light, $\hat{\sigma}_{x,z}$ are the Pauli matrices.

The incident Dirac particle is incident from the left and passes three regions denoted by I, II, III, respectively. The Floquet solution of eq. (2) for a given incident energy E can be written as

$$\Phi^i(x,t) = \sum_{n=-\infty}^{+\infty}\sum_{l=-\infty}^{+\infty}\left[a_l^i\begin{pmatrix}1\\ \dfrac{p_l c}{E_l - V_0 + mc^2}\end{pmatrix}e^{ip_l x} + b_l^i\begin{pmatrix}1\\ \dfrac{-p_l c}{E_l - V_0 + mc^2}\end{pmatrix}e^{-ip_l x}\right]J_{n-l}\left(\frac{V}{\hbar\omega}\right)e^{-iE_n t/\hbar}, \quad (4)$$

where J_n is the Bessel function of the first kind, a_l^i and b_l^i are constant coefficients. In the barrier region $i = II$, p_l is $p_l = \mathrm{sgn}(E_l - V_0)\left[(E_l - V_0)^2 - m^2c^4\right]^{1/2}/c$ and $E_l = E + l\hbar\omega$. Outside the barrier region $i = I, III$, p_l is $p_l' = \mathrm{sgn}(E_l)\left[(E_l)^2 - m^2c^4\right]^{1/2}/c$ and $J_{n-l}(\frac{V}{\hbar\omega}) = \delta_{ln}$. The Dirac particles incident to the driven potential will be scattered inelastically into Floquet sidebands (channels) with energy spacing $\hbar\omega$ according to $E_n = E + n\hbar\omega$. The mode of $E_n < 0$ is an evanescent mode and the corresponding sideband is called evanescent sideband because such a mode with imaginary p_n' cannot propagate [15]. Using the continuity of Φ at the interfaces $x = -a/2$ and $a/2$, the scattering matrix for the single potential barrier is given by [15]

$$\begin{pmatrix} b^I \\ a^{III}\end{pmatrix} = S\begin{pmatrix} a^I \\ b^{III}\end{pmatrix} = \begin{pmatrix} r & t' \\ t & r'\end{pmatrix}\begin{pmatrix} a^I \\ b^{III}\end{pmatrix}, \quad (5)$$

where r and t are matrices whose elements denote the probability amplitudes of reflection and transmission, respectively, for modes in which the Dirac particle is incident from the left (region I). For instance, the matrix element t_{nl} is the probability amplitude of transmission for a Dirac particle incident from channel l on the region I to appear at a channel n on the region III. r' and t' describe the scattering process incident from the right (region III). The total Dirac-particle transmission probabilities for incident E are given by

$$T = \sum_{n=0}^{+\infty}\frac{p_n'/\left(E_n + mc^2\right)}{p_0'/\left(E_0 + mc^2\right)}\left|t_{n0}\right|^2. \quad (6)$$

For the static quantum barrier in the absence of oscillating field the continuum region $E > mc^2$ corresponds to continuum states of free Dirac particles. The quantized spectrum of the bound state and the extended state in the energy region $-mc^2 < E < mc^2$ is given by the transcendental equations based on the continuity condition

$$\tan\frac{pa}{2} = -\mathrm{sgn}(E)\sqrt{\frac{(mc^2 - E)(V_0 - E - mc^2)}{(mc^2 + E)(V_0 - E + mc^2)}}, \quad (7)$$

$$\tan\frac{pa}{2} = \mathrm{sgn}(E)\sqrt{\frac{(mc^2 + E)(V_0 - E + mc^2)}{(mc^2 - E)(V_0 - E - mc^2)}}, \quad (8)$$

where $p = \sqrt{(V_0 - E)^2 - m^2c^4}/c$. The discrete energy spectrum depends not only on V_0, a and mc^2 but also on the sign of the energy E. It is corresponding to the bound state for $E > 0$ and the extended state for $E < 0$. The positive-energy solutions are the same as the results of refs. [16,17] and the corresponding wave function is a bound state, while in general the negative-energy solutions have been ignored before because their wave functions are extended states.

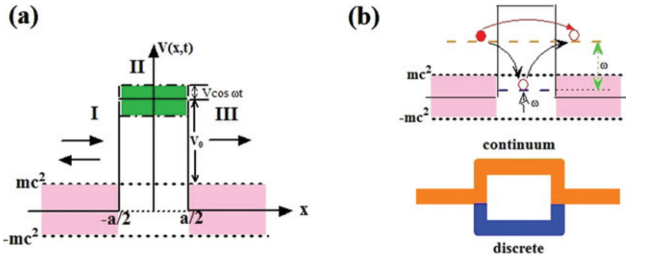

Fig. 1: (Color online) (a) Schematic diagram of the model for Dirac particle transmission through a single potential barrier under the applied oscillation field $V\cos(\omega t)$. (b) The mechanism diagram of Fano resonance from the interference between the continuum band and the discrete level.

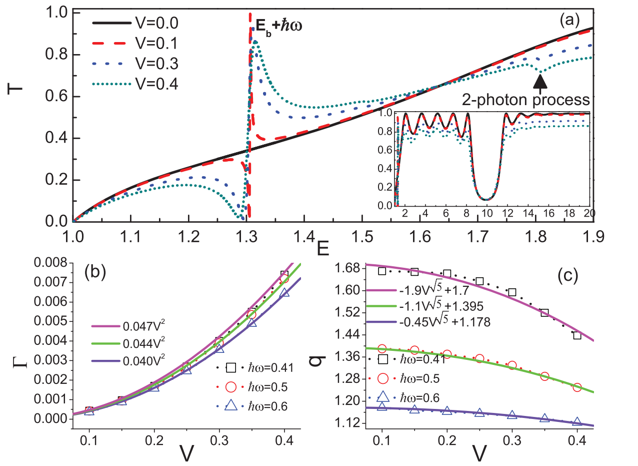

Fig. 2: (Color online) The systems parameters $V_0 = 10$, $a = 2$, and $mc^2 = 1$. (a) The transmission coefficient T for low frequency $\hbar\omega = 0.5 < mc^2$ as a function of incident energy. (b) and (c): the linewidth Γ and asymmetry parameter q as a function of weaker oscillation amplitude V for different frequency, respectively. All kinds of blank shape come from the formula of the Fano line; color solid lines $\Gamma \propto V^2$, $q \propto -V^{\sqrt{5}}$.

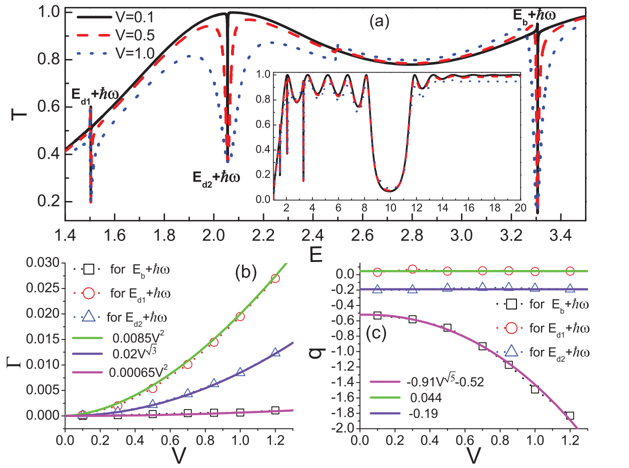

Fig. 3: (Color online) The systems parameters $\hbar\omega = 2.5$, $V_0 = 10$, $a = 2$, and $mc^2 = 1$. (a) The transmission coefficient T for high frequency $\hbar\omega > mc^2$ as a function of incident energy. (b) and (c): the linewidth Γ and asymmetry parameter q as a function of weak oscillation amplitude V, respectively. All kinds of blank shape come from the formula of the Fano line; the magenta solid line $\Gamma \propto V^2$, $q \propto -V^{\sqrt{5}}$ for normal Fano resonance; the violet solid line $\Gamma \propto V^{\sqrt{3}}$, $q \approx$ const and the green line $\Gamma \propto V^2$, $q \approx$ const for anomalous Fano resonance.

Anomalous Fano resonance. – We study numerically the scattering of a single incident wave through an oscillating quantum barrier and calculate the transmission coefficients. The width and strength of a static potential barrier are set as $a = 2$ and $V_0 = 10$, respectively. The minimum number of sidebands needed in the sum of eq. (6) depends on the oscillation amplitude of the potential. According to ref. [18], we should take $N > V/\hbar\omega$.

In the absence of oscillating field, the transmission coefficient in eq. (6) changes to $T = \frac{4\eta^2}{[4\eta^2+(1-\eta^2)^2\sin^2(pa)]}$ [19], where $\eta = \sqrt{\frac{(V_0-E+mc^2)(E+mc^2)}{(V_0-E-mc^2)(E-mc^2)}}$, and the transmission has smooth resonant peaks described as Klein tunnelling which is enhanced for the barrier if $pa = N\pi$, corresponding to the energy of Klein peaks $E_N = V_0 - \sqrt{m^2c^4 + \left(\frac{N\pi}{a}\right)^2}$. The Klein tunneling due to conservation of particle-antiparticle in the Dirac system is shown as the solid black line of fig. 2(a).

In the presence of oscillating field, the bound state of the potential barrier may provide the discrete channel of scattering required by the Fano resonance as shown in fig. 1(b). Once the energy difference between the incident Dirac particles and the bound states in the barrier is equal to the energy of one or more photons ($E = E_b + n\hbar\omega$), transmission resonance occurs. As shown in fig. 2(a), the Fano resonance appears and the resonance energy satisfies the relation $E = E_b + \hbar\omega$ for low amplitude of the oscillating field, for instance for $V = 0.1$ the resonance energy is $E = 1.306$, corresponding to bound states with positive energy $E_b = 0.806268$ for the static quantum barrier from eq. (7) and eq. (8). With the increase of the oscillation amplitude, a weaker two-photon–assisted Fano resonance appears in the energy region. These results are similar to the ones of the nonrelativistic electron [20], the relativistic massless Dirac particles [12] and the massive Dirac particles [14].

With the increase of the oscillation amplitude, the total transmission including Klein tunneling and Fano resonance is suppressed, and the width of the Fano resonance increases as V increases. Using the formula of the Fano line[1], the linewidth Γ and the asymmetry parameter q of the Fano line as a function of the oscillation amplitude V can be obtained, and plotted in fig. 2(b) and fig. 2(c), respectively. It is found that the linewidth is approximately proportional to the square of the oscillation strength, *i.e.*, V^2, which is the same as the result of ref. [2], and the asymmetry parameter is approximately proportional to $-V^{\sqrt{5}}$ for weak oscillation.

In the above study the frequency is low and $\hbar\omega < mc^2$, in the following we turn to discuss the phenomena for the high frequency, $\hbar\omega > mc^2$. The transmission coefficient as a function of incident energy for high frequency is plotted in fig. 3(a). The results show that three Fano resonances appear, one of them is corresponding to the bound state with the bound energy E_b, *i.e.*, the incident energy $E = E_b + \hbar\omega$; the other two new ones appear at $E = 1.50329$ and 2.05535 which happen to correspond to one-photon processes from the negative-energy solutions ($E_{d1} = -0.444681$ and $E_{d2} = -0.996712$) of eq. (7) and

[1] $\frac{p_{\max}}{1+\Delta+q^2}\left[\frac{(\epsilon+q)^2}{\epsilon^2+1}+\Delta\right]$ with $\epsilon = 2(E-E_0)/\Gamma$ and $\Delta = \frac{(1+q^2)p_{\min}}{p_{\max}-p_{\min}}$. E_0, Γ and q are the resonant energy, linewidth and asymmetry parameter, respectively. $p_{\min}$ and $p_{\max}$ are the minimum and maximum of the Fano resonance peak.

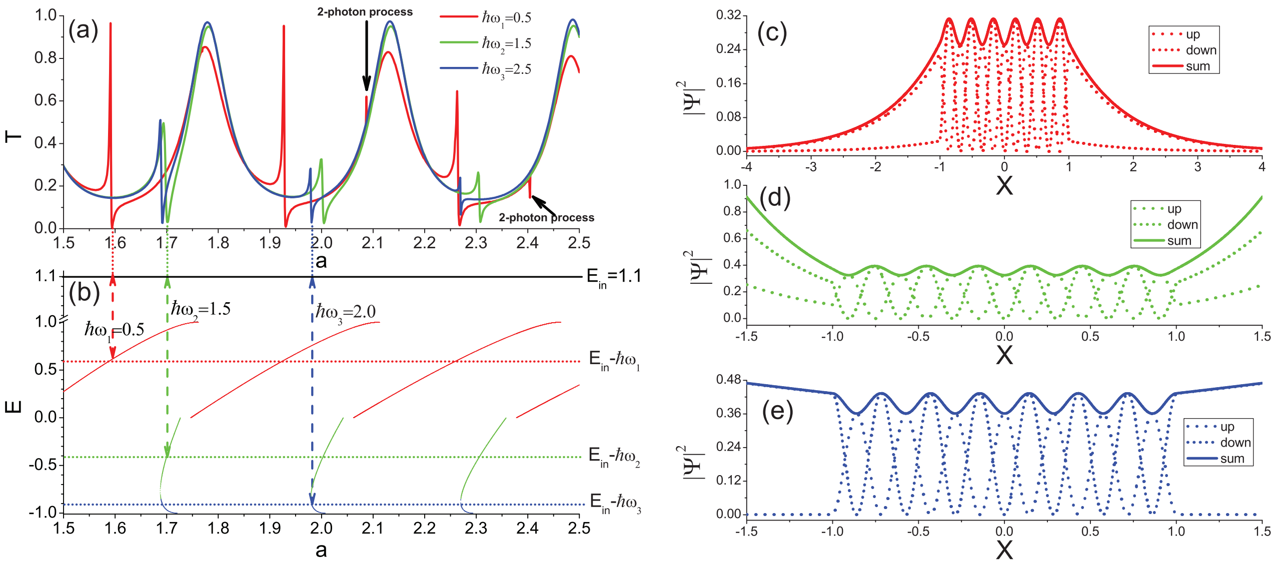

Fig. 4: (Color online) For $V_0 = 10$ and $mc^2 = 1$. (a) The transmission coefficient T as a function of the width, a, of the barrier for given incident energy $E_{in} = 1.1$, and $V = 0.3$, $\hbar\omega_1 = 0.5$, $\hbar\omega_2 = 1.5$, $\hbar\omega_3 = 2.0$. (b) The energy spectrum *vs.* the width, a, of the barrier. The red line shows the solutions of bound states, the green line and the blue line stand for the solutions of extended states. Panels (c)–(e) are the wave functions of the bound state and extended states for $a = 2$. The "up" dotted line shows the up component, the "down" dashed line indicates the down component and the "sum" solid line stands for the sum of the up and down components.

eq. (8), that is to say, $E = E_{dj} + \hbar\omega$ $(j = 1, 2)$. The two new ones belong to supercritical resonances because the incident particle energy with positive-energy states matches a negative-energy state's frequency.

For the high-frequency case, the linewidth Γ and the asymmetry parameter q as a function of the weaker oscillation amplitude V are plotted in fig. 3(b) and fig. 3(c). We can find that the linewidths increase with power laws of V, approximately proportionally to V^2 for E_b and E_{d2}, and to $V^{\sqrt{3}}$ for E_{d1}. We can also see that the coefficients of power laws for E_{dj} are much larger and the linewidths for the two extended states grow rapidly. More intriguingly, the asymmetry parameter is approximately proportional to $-V^{\sqrt{5}}$ for the bound state, while the asymmetry parameters for the two extended states are approximately equal to constants for different oscillation amplitudes. This can be used to distinguish between the Fano resonance of the bound state and that of extended states in experiment.

It is well known that the appearance of Fano resonance is dependent on the energy spectrum of the static potential barrier. The incident Dirac particles can emit photons and drop to discrete levels embedded in the potential barrier, then jump to the incident channel by absorbing photons. In fig. 4(a) and fig. 4(b) we plot the transmission coefficient for given incident energy $E_{in} = 1.1$ and the energy spectrum as a function of the potential width a, respectively. It is seen that for the low frequency, $\hbar\omega_1 = 0.5$, normal Fano resonances appear at the positons with $E_{in} = E_b + \hbar\omega_1$, and the weak two-photon process occurs at $E_{in} = E_b + 2\hbar\omega_1$, which are the same as the result of ref. [14]. The bound wave function of the discrete energy level E_b is shown in fig. 4(c). For the high-frequency case, $\hbar\omega_2 = 1.5 > mc^2(= 1)$, new Fano resonances appear at the positions with $E_{in} = E_{d1} + \hbar\omega_2$ (see green line of fig. 4(a)), and the wave function corresponding to E_{d1} is an extended wave function as shown in fig. 4(d). Another kind of new Fano resonance occurs at the position with $E_{in} = E_{d2} + \hbar\omega_3$ at $\hbar\omega_3 = 2.0 > mc^2$, denoted by the blue line of fig. 4(a), and the corresponding wave function of the discrete energy level E_{d2} is shown in fig. 4(e).

The new-kind Fano resonance (here denoted as anomalous Fano resonance) for the high-frequency cases results from the interference between a continuum band and embedded discrete levels with extended wave functions. We know that the extended solutions for the Dirac equation always exist [21], but the discrete levels with extended wave function have always been abandoned before since one believes the wave function of the discrete level should be localized, and so far no effect caused by the extended states for the Dirac equation has been observed. However, here we find that the Fano resonances correspond to such discrete levels. Indeed, the incident Dirac particle does not emit and absorb real photons for dropping to the extended states and jumping back to the continuum respectively, hence the anomalous Fano resonance just occurs with a virtual process by virtual photons.

Discussions and conclusions. – We have investigated theoretically the property of the massive Dirac particle transmission over a barrier with an oscillating field. For the first time we find the anomalous Fano resonance by studying the asymmetry parameters of Fano resonance, which are quite different from those of the normal Fano resonance. For the anomalous Fano resonance the asymmetry parameters are approximately equal to a constant with the increase of the oscillation amplitude, while for the normal Fano resonance the asymmetry parameters are approximately proportional to $-V^{\sqrt{5}}$. From the point of view of the physical mechanism the anomalous Fano resonance arises from the interference between an extended state and the continuum state, rather than from the interference between the traditional bound state and the continuum state.

In general the one-photon–assisted process plays a major role in the occurrence of the Fano resonance. For nonrelativistic particle and relativistic Dirac particle without mass, Fano resonance occurs when $E_{in} = E_b + \hbar\omega$. However, for massive relativistic Dirac particle there is a forbidden band from $-mc^2$ to mc^2, therefore the energy of the incident particle must be not less than mc^2. Hence there should be a threshold for frequency, *i.e.*, $\hbar\omega_c = mc^2 - E_{b(dj)}$, for the occurrence of Fano resonance, and Fano resonance may occur only for $\hbar\omega > \hbar\omega_c$. The energy E_{dj} is less than zero, therefore the occurrence of the anomalous Fano resonance need satisfy $\hbar\omega > \hbar\omega_c (> mc^2)$. Such a high frequency is corresponding to γ-rays for real electron which is very difficult to be implemented in experiment. However, the gap can be tuned generally in experiment for bilayer graphene [22–24], Fermi cold atoms in honey comb lattice [25] and photonic simulation in subwavelength materials [26]. For graphene the energy gap is corresponding to infrared light while for cold atom and photonic simulation they are corresponding to microwave, therefore the condition may be easier to be satisfied in experiment. On the other hand, although our model is a simple rectangular potential barrier, the negative-energy solutions of extended states do not depend on the choice of potential, so it causes no loss of generality. Thus the novel physical phenomena of anomalous Fano resonance may be observed experimentally in graphene, ultra-cold atoms, subwavelength materials, or other massive Dirac systems.

* * *

This work is supported by the National Fundamental Research Program of China (Contracts No. 2013CBA01502, No. 2011CB921503, and No. 2013CB834100), the National Natural Science Foundation of China (Contracts No. 11374040, No. 11274051 and No. 11304281), and the Zhejiang Education Department (Grant No. Y201225191).

REFERENCES

[1] Fano U., *Phys. Rev.*, **124** (1961) 1866.

[2] Miroshnichenko A. E., Flach S. and Kivshar Y. S., *Rev. Mod. Phys.*, **82** (2010) 2257.

[3] Lukyanchuk B., Zheludev N. I., Maier S. A., Halas N. J., Nordlander P., Giessen H. and Chong C. T., *Nat. Mater.*, **9** (2010) 707.

[4] Polini M., Guinea F., Lewenstein M., Manoharan H. C. and Pellegrini V., *Nat. Nanotechnol.*, **8** (2013) 625.

[5] Schrödinger E., *Sitzungsber. Preuss. Akad. Wiss. Phys. Math. Kl.*, **24** (1930) 418.

[6] Zhang X. D., *Phys. Rev. Lett.*, **100** (2008) 113903.

[7] Katsnelson M. I., Novoselov K. S. and Geim A. K., *Nat. Phys.*, **2** (2006) 620.

[8] Tang T. T., Zhang Y., Park C. H., Geng B., Girit C., Hao Z., Martin M. C., Zettl A., Crommie M. F., Louie S. G., Shen Y. R. and Wang F., *Nat. Nanotechnol.*, **5** (2010) 32; Liu Z., Lu X., Peng P., Wu W., Pei S. S., Yu Q. and Bao J., *Phys. Rev. B*, **82** (2010) 155435.

[9] Kuzmenko A. B., Benfatto L., Cappelluti E., Crassee I., van der Marel D., Blake P., Novoselov K. S. and Geim A. K., *Phys. Rev. Lett.*, **103** (2009) 116804; Li Z., Lui C. H., Cappelluti E., Benfatto L., Mak K. F., Carr G. L., Shan J. and Heinz T. F., *Phys. Rev. Lett.*, **108** (2012) 156801; Lui C. H., Cappelluti E., Li Z. and Heinz T. F., *Phys. Rev. Lett.*, **110** (2013) 185504.

[10] Cappelluti E., Benfatto L. and Kuzmenko A. B., *Phys. Rev. B*, **82** (2010) 041402; Cappelluti E., Benfatto L., Manzardo M. and Kuzmenko A. B., *Phys. Rev. B*, **86** (2012) 115439.

[11] Seridonio A. C., Siqueira E. C., Souza F. M., Machado R. S., Lyra S. S. and Shelykh I. A., *Phys. Rev. B*, **88** (2013) 19512.

[12] Lu W. T., Wang S. J., Li W., Wang Y. L., Ye C. Z. and Jiang H., *J. Appl. Phys.*, **111** (2012) 103717.

[13] Sinha C. and Biswas R., *Appl. Phys. Lett.*, **100** (2012) 183107; Biswas R. and Sinha C., *J. Appl. Phys.*, **114** (2013) 183706.

[14] Szabó L. Z., Benedict M. G., Czirják A. and Földi P., *Phys. Rev. B*, **88** (2013) 075438.

[15] Li W. and Reichl L. E., *Phys. Rev. B*, **60** (1999) 15732.

[16] Greiner W., Muller B. and Rafelski J., *Quantum Electrodynamics of Strong Fields* (Springer, Berlin) 1985.

[17] Calogeracos A., Dombey N. and Imagawa K., *Yad. Fiz.*, **159** (1996) 1331 (*Phys. At. Nucl.*, **159** (1996) 1275).

[18] Bulgakov E. N. and Sadreev A. F., *J. Phys.: Condens. Matter*, **8** (1996) 8869.

[19] Dosch H. G., Jensen J. H. and Muller V. F., *Phys. Norv.*, **5** (1971) 151.

[20] Zhang C. X., Nie Y. H. and Liang J. Q., *Phys. Rev. B*, **73** (2006) 085307.

[21] Shen S. Q., Shan W. Y. and Lu H. Z., *SPIN*, **1** (2011) 33.

[22] Ohta T., Bostwick A., Seyller T., Horn K. and Rotenberg E., *Science*, **313** (2006) 951.

[23] Oostinga J. B., Heersche H. B., Liu X., Morpurgo A. F. and Vandersypen L. M. K., *Nat. Mater.*, **7** (2008) 151.

[24] Castro Eduardo V., Novoselov K. S., Morozov S. V., Peres N. M. R., Lopes dos Santos J. M. B., Nilsson J., Guinea F., Geim A. K. and Castro Neto A. H., *Phys. Rev. Lett.*, **99** (2007) 216802.

[25] Tarruell L., Greif D., Uehlinger T., Jotzu G. and Esslinger T., *Nature*, **483** (2012) 302.

[26] Tan W., Sun Y., Chen H. and Shen S. Q., *Sci. Rep.*, **4** (2014) 3842.